Iranian Journal of Materials Science and Engineering, Vol. 18, Number 2, June 2021
RESEARCH PAPER

Characterization of the Early Surface Films Dynamically Formed on Molten AZ91D and AM60B Alloys under Different Atmospheres: A Comparative Study

Alireza Mirak*

* *alireza.mirak@gmail.com*
* Faculty of Materials and Manufacturing Technologies, Malek-Ashtar University of Technology, Tehran, Iran

Received: September 2019 **Revised: June 2020** **Accepted: December 2020**
DOI: 10.22068/ijmse.1570

Abstract: *In the present study, the early stages of the surface oxidation and fluoridation of liquid AZ91D and AM60B alloys under ultra-high purity (UHP) argon, dry air, and air mixed with two different protective fluorine-bearing gases were studied. The chemical composition, morphology and thickness of the surface films formed inside the trapped bubbles were characterized by SEM equipped with EDS analysis. It is found that the molten AM60B alloy is more sensitive to impurities under UHP argon gas than AZ91D alloy. Under dry air atmosphere, the entire surface of molten AZ91D alloy is covered with an oxide layer and thinner thickness than the surface film formed on AM60B alloy which has rough surface exhibiting granular growth in later stages of oxidation. The EDS analysis shows that the film chemistry is mainly composed of Mg, Al and O elements. Under fluorine-bearing gas/air mixtures with either SF_6 or HFC-R134a at 3.5%vol., a fresh surface film formed with a flat and dense morphology with a uniform thickness consisting of Mg, F, Al and O elements. It is observed that there is a lower O:F intensity ratio in the surface film formed on the molten AZ91D alloy under 1,1,1,2-tetra-fluoroethane (HFC-R134a) mixed with dry air compared to the AM60B alloy under both air/ R134a and air/SF_6 mixtures which shows a higher fluorine concentration in the surface film a leading to a better oxidation resistance.*

Keywords: *Molten AZ91D and AM60B alloys, fresh Surface film, Oxidation, Fluoridation*

1. INTRODUCTION

Magnesium alloys are being increasingly used in the light-weight structural applications due to their excellent physical and mechanical properties, such as high specific strength, rigidity, low density and good damping capacity [1]. However, molten magnesium alloys have a high affinity for oxygen and a high vapor pressure which accordingly makes it necessary to protect the melt from oxidation and burning during the melting and casting processes.

In order to process molten magnesium safely and efficiently, considerable effort has been made to study the oxidation behavior of molten magnesium alloys and to change the nature of the surface film over the melt surface such that it acts protectively. Consequently, it is known that the alloy and cover gas compositions have a direct effect on the various morphologies and chemistries of the surface films formed [2, 3].

During the casting process, the molten metal is in motion rather than remaining stagnant and fresh surfaces are created and exposed to the surrounding atmosphere. Therefore, the oxide layer is continually subjected to deformation forces and may buckle or fold under compression. Since the oxide film is expected to have little or no plasticity, it may tear when subjected to excessive tension thus allowing fresh oxidation to occur. Clearly, both fresh as well as older, thicker oxide films can exist in a casting and the nature of these oxides can have a strong influence on the mechanical properties of castings [4]. Experiments, which will be detailed later, have been carried out on the oxidation behavior of molten magnesium alloys in stagnant melts held isothermally.

The protection afforded by SF_6-containing atmospheres over the melts of pure magnesium and AZ91B alloy has been noted, because it allows the formation of a thin, coherent and stable film on the melt surface [5]. Aarstad [6] used various techniques to study the surface of molten magnesium which was held isothermally and protected by SF_6. He found that the thickness of the film varied between 0.3 and 1 μm due to increases in melting temperature and holding time.

Some researchers have studied the use of air/R134a (1,1,1,2-tetra-fluoroethane) for magnesium melt protection. They found that it can provide excellent protection while also ameliorating the

[DOI: 10.22068/ijmse.1570]

serious greenhouse effect caused by of SF_6 in the atmosphere [7, 8]. Ricketts and Cashion [9] have reported that HFC-R134a also provides greater thermal stability at high temperature than SF_6 thus prolonging its protective benefits.

Most alloying elements do not contribute to the protection of molten Mg alloys. At present, only Be and Ca (or CaO) are considered as providing any protection [10, 11]. The effect of Al content in AZ91 alloy is expected to cause some difference in oxidation in both liquid [12] and solid state [13]. Liu et al. [14] examined the oxidation rates and film compositions of molten pure magnesium and AZ91D alloy at 760ºC under different concentrations of HFC-R134a mixed with dry air and found that the aluminum-containing AZ91 alloy was more resistant to oxidation than pure Mg.

In the previous work, we have characterized the early stages of surface oxidation of pure Mg under dry air and air/SF_6 and air/HFC-R134a mixtures by SEM and XRD techniques. Under fluorine bearing gases, the surface films appear uniform and largely undamaged. Also under dry air, the entire surface is covered with oxide film of varying thickness, with a wrinkled and folded morphology [15].

The present research was conducted in order to extend the understanding of the early stages of surface oxide/fluoride formation and growth under conditions similar to those occurring during casting or melt handling processes. The aim is to compare the morphology and composition of these oxide films, formed under different atmospheres, namely, UHP argon, dry air, air/SF_6 and air/HFC-R134a mixtures. This was carried out via the introduction of different bubble gases into solidifying melts in a permanent mould. Characterization of the formed surface film (chemical and morphological) was carried out by SEM and EDS investigation techniques.

2. EXPERIMANTA PROCEDURES

The AZ91D and AM60B alloys, which were used in this research, were melted at 650 ± 5ºC in a mild steel crucible using an electrical resistance furnace. The chemical compositions of the two alloys are shown in Table 1. This occurred under the protection of a SF_6/air mixture.

Table 1. Chemical compositions of alloys examined by argon plasma mass spectrometer

	Al	Zn	Mn	Si	Fe	Ni	Mg
AZ91D	8.9	0.59	0.34	0.03	0.002	0.0005	Bal.
AM60B	5.5	0.22	0.5	0.05	0.005	0.002	Bal.

All values in are wt.%.

Each melt was cast into a permanent steel mould (preheated to 450 ± 10ºC) to produce a simple plate casting via a bottom gating system. The base of the casting plate was 14 mm thick, tapering linearly to 7 mm near the top.

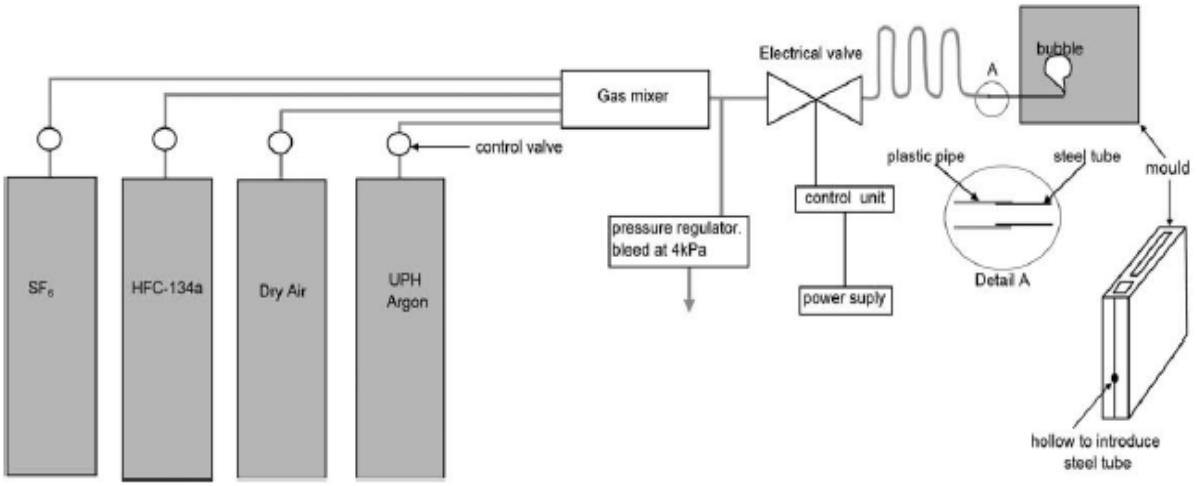

Fig. 1. Schematic diagram of the experimental arrangement

[DOI: 10.22068/ijmse.1570]

A disposable thin stainless steel tube (1 mm ID, 1.6 mm OD) was inserted horizontally into the base of the mould cavity. Figure 1 shows the experimental arrangement used for generation of the fresh surface films under different atmospheres.

When changing gas mixtures, the gas lines were purged to remove traces of previous gases. Before each casting, the solenoid valve was opened for approximately 5 min to flush the gas feed line. The purge gas flow was stopped just before the casting was poured and as soon as the casting cavity was filled, the solenoid was manually operated for about 2s to let in a small flow of gas to create bubbles within the casting plates during solidification. The following gas mixtures were used: ultra-high purity (UHP) argon, industrial dry air, 3.5% SF_6 in dry air, and 3.5% HFC-R134a in dry air. The feed gas compositions and their significant impurities are as follows:

(i) UHP argon, min 99.999%, O_2 < 1 ppm, H_2O < 2 ppm;
(ii) Industrial dry air, 20.9% O_2, H_2O typically 25 ppm;
(iii) SF_6, min 99.8%, CF4 < 1000 ppm, H_2O < 120 ppm, typical acidity (HF) 0.3 mg/kg, hydrolysable fluorides 1 mg/kg;
(iv) 1, 1, 1, 2 tetra-fluoroethane (HFC-R134a), min 99.5%, H_2O < 10 ppm, acidity (HF) 1 ppm, other refrigerants 0.5 ppm.

For each experimental condition, four plate castings were made. X-ray radiography was used to determine the exact locations of ideal bubble specimens. The bubble-melt interfaces were then extracted from the plates by sectioning techniques. These specimens represented the early surface films formed under carefully controlled reaction conditions at short exposure times. The morphologies of these internal surface oxide/fluoride films were examined using a JEOL 6460 LA SEM, while the chemical constituents of the films were determined using an attached EDS spectrometer with an ultra-thin window suitable for light element analysis. All analyses were carried out at 12 keV.

For the measurement of film thickness, the procedure was to initially prepare calibration curves of Mg/O and Mg/F X-ray intensity ratios against film thickness for various film materials (e.g. as seen in Figures 3 and 4 in Ref. 15). These curves were produced by Monte-Carlo simulation of X-ray generation under an electron beam using the Casino software package. The detector efficiency for each element of interest (Mg, F and O) was scaled by comparing the predicted and measured responses for known standards materials such as pure Mg, MgO, CaF_2 and dolomite. For more details on the film thickness measurement technique, the reader is referred to the full description given elsewhere. [15]

3. RESULTS AND DISCUSSION

3.1. Surface film X-ray analysis – Qualitative

Figure 2 shows the normalized EDS spectra from general areas which the majority of the bubble surfaces of AZ91D and AM60B magnesium alloys. The chemical characteristics of the surface film can be seen distinctly for each gas condition. As expected, the surface films formed under dry air atmosphere are composed of Mg, Al, O and C as the main elements. Meanwhile the fluorine peak is a fixed characteristic of the surface films in both alloys formed under fluorine bearing gases. As can be seen in Fig. 2a, the spectra show a strong correlation between oxygen and fluorine content in AZ91D alloy particularly under the SF_6 atmosphere. The higher level of oxygen observed under the dry air atmosphere in AM60B alloy compared to the other atmospheres is evident in Fig. 2b. The spectra also indicate that sulphur is present in the surface films formed under SF_6 atmosphere. This can be attributed to the amorphous structure of MgS or to small amounts of elemental sulphur present in the films. Aluminum is identified as a major element in the surface films and both sub-surface alloys. For both alloys, the highest and lowest Al intensity peaks are attributed to HFC-R134a and (UHP) argon respectively and this leads to a higher reaction of aluminum with fluorine under HFC-R134a than other atmospheres. Silicon is the major impurity source in the ingot, at approximately 0.03 wt.%. It is assumed that the levels of Si observed under the argon, air and HFC-R134a atmospheres are consistent with this, but in molten AM60B alloy, the peak intensity under dry air gas is consistently higher than the other gases, suggesting some minor preferential diffusion to the surface under air atmosphere. The carbon peak appears

[DOI: 10.22068/ijmse.1570]

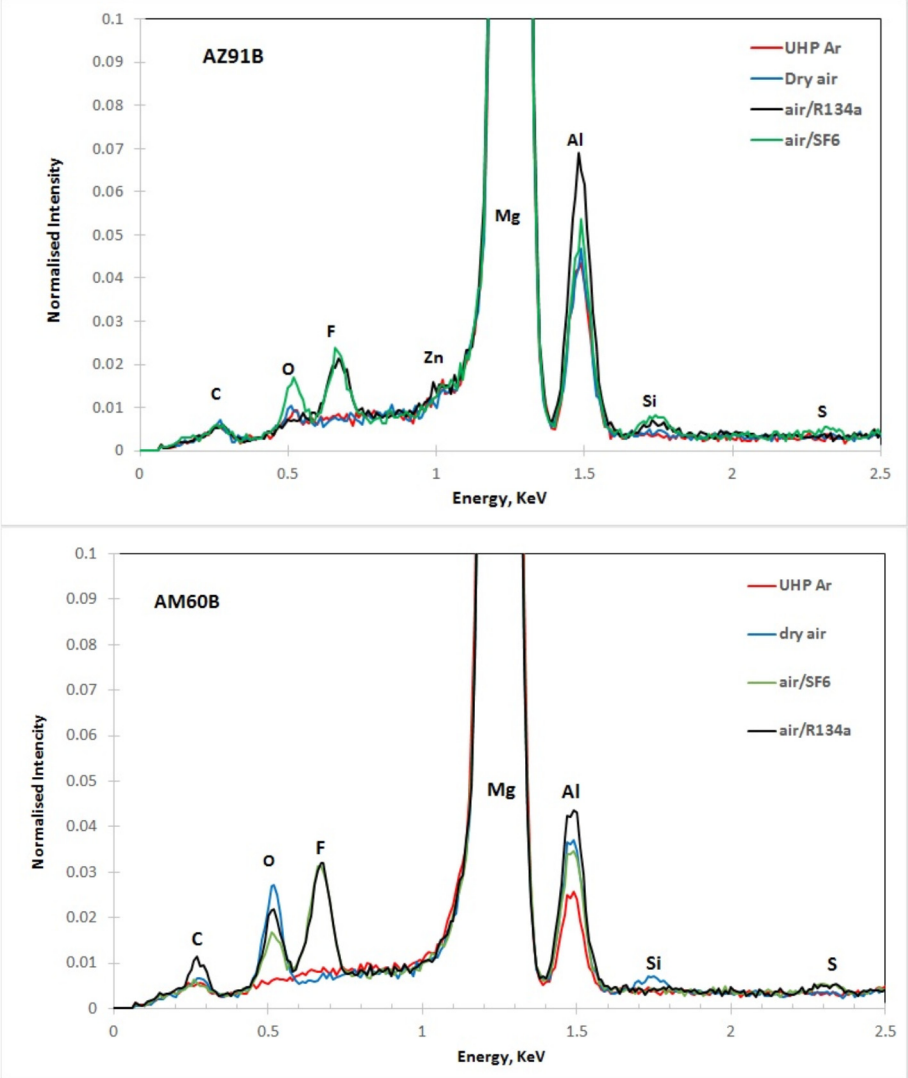

Fig. 2. Representative EDS spectra of the early surface films of bubbles formed in molten AZ91D alloy and AM60B alloy using different bubble gas atmospheres. These spectra have been normalized to the Mg K_α peak and the relevant peaks identified for AZ91D and AM60B.

significant; however there was an evidence of higher carbon intensity when the bubble contained HFC-R134a, compared to other gases in AM60B alloy.

3.2. Surface film observations under SEM

Figures 4 to 7 show various SEM images of the physical structure of the early surface films formed on the (inside) surfaces of the bubbles entrapped in molten alloys under different atmospheres. Ranges of macro- and micro-structures are apparent. The sub-surface alloy microstructure appears to be cellular/dendritic, with the growth direction generally from the mould wall towards the bubble. The microstructure consists of primary α-Mg and lamellar structure of Mg-Al eutectic phases which are distributed along the grain boundaries. There are also coarse intermetallic particles present, e.g. Alx Mny where x and y are primarily dependent on the composition of the base alloy (see Fig. 3). The structures and morphology of the surface films formed under different atmospheres are described and discussed in more details in the following sub-sections.

3.2.1. UHP argon

Figure 4 presents the typical morphology of the inner bubble surface films formed under UHP argon atmosphere. As it can be seen in Fig. 4a

[DOI: 10.22068/ijmse.1570]

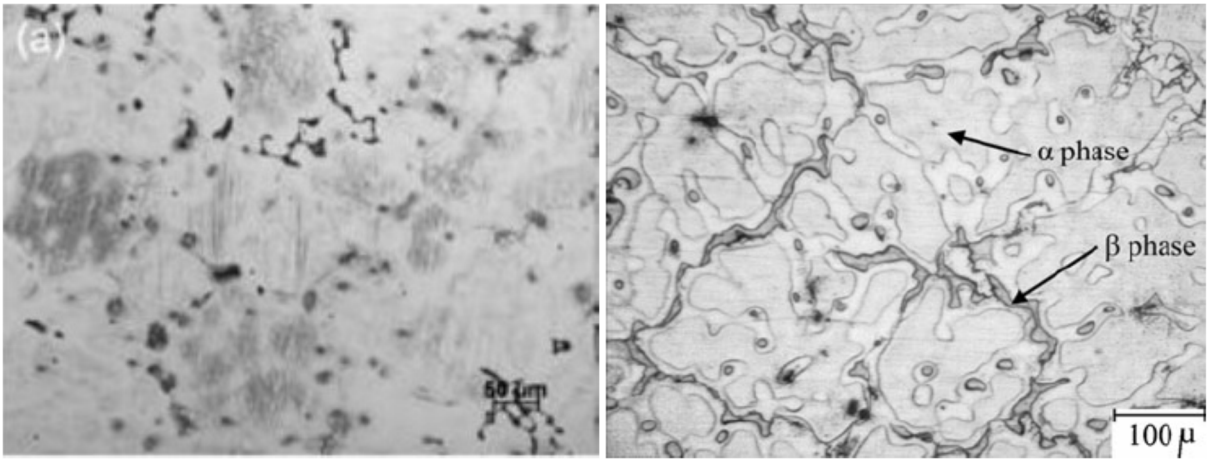

a **b**

Fig. 3. Optical images showing general view of the microstructure of a) AM60B and b) AZ91D alloys

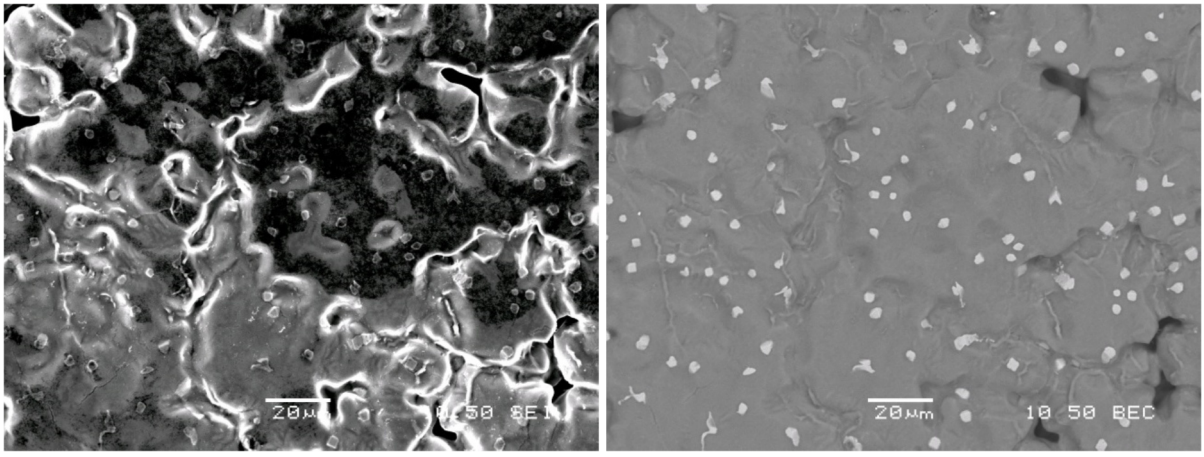

a **b**

Fig. 4. SEM image from the general view of the inner surface of an entrapped UHP argon bubble in AZ91D alloy a) SE image from surface film, b) BE image from the same area showing Al-Mn intermetallic particles.

due to non-reactivity of the UHP-Ar with the surface of the molten AZ91D alloy, the majority of the surface is relatively clean (greyish colour in Fig.4a) and the eutectic patches (Mg and $Mg_{17}Al_{12}$) were formed around the dendrites with a dark planar oxide film observed. Also there are scattered spots which are richer in oxygen which are presumed to be the heterogeneous nucleation sites of oxide. These spots may have been favoured by the very low oxygen partial pressure and/or grew laterally until the oxygen is exhausted. The white nodular phases with 2 μm range size shown in Fig. 4b are identified as Al-Mn intermetallic particles.

The surface film morphology of the bubble formed in the solidified AM60B alloy under UHP argon gas is shown in Fig. 4. As indicated, there is an unreacted surface (A marked in Fig.5a) and also some ridge shaped areas which are identified as patches of oxide (B marked in Fig. 5a). A magnified SEM image from a thick oxide patch is shown in Fig. 5c. and reveals a folded and sponge-like morphology with many cracks and holes. It appears that the molten AM60B alloy is more sensitive to impurities under UHP Ar gas than AZ91D alloy.

The main elements in the early surface film are Mg, Al and small quantities of O according to EDS analysis on the majority of the surface and bulk alloy (e.g. Fig. 2). From X-ray analyses of (from) the cleaner parts of Fig. 4 and 5, the oxide films were calculated to be less than 20 nm thick according to the calibration graph shown in Fig. 3 in Ref. 15. Consequently, this thickness is assumed to represent the upper limit of subsequent oxide growth at room temperature.

[DOI: 10.22068/ijmse.1570]

The rough oxide patch areas in AM60B alloy averaged 100 nm thicknesses (B marked area in Fig. 5c).
The main source of oxygen is most likely from the residual air in the steel tube which had not been fully purged prior to casting. The presumed inertness of the UHP argon atmosphere is clearly sensitive to small amounts of entrapped air such that the growth rate of MgO film on Mg base alloy is equivalent to the oxidation rate observed under dry air atmosphere.
It is therefore understood that the use of UHP argon is limited for prevention of oxidation of molten Mg alloy due to the high vaporization of Mg near its melting point.

An experiment was carried out on oxidation of Mg alloy in the molten state which showed that the inert gas did not prevent evaporation and this led to an increased oxidation rate in the early stage (less than 10 second) but that at longer times, the oxidation rate of Mg alloy decreased under argon atmosphere [15]

3.2.2. Dry air

Figure 6 shows the typical morphologies of the fresh surface oxide films dynamically formed under industrial dry air atmosphere in the bubbles trapped in the solidifying AZ91D (Fig. 6a,b) and AM60B alloys (Fig. 6c,d) at the earlier stage of oxidation. As it can be seen, in the AZ91D alloy, the entire surface is covered with an oxide layer. Also, some granular regions

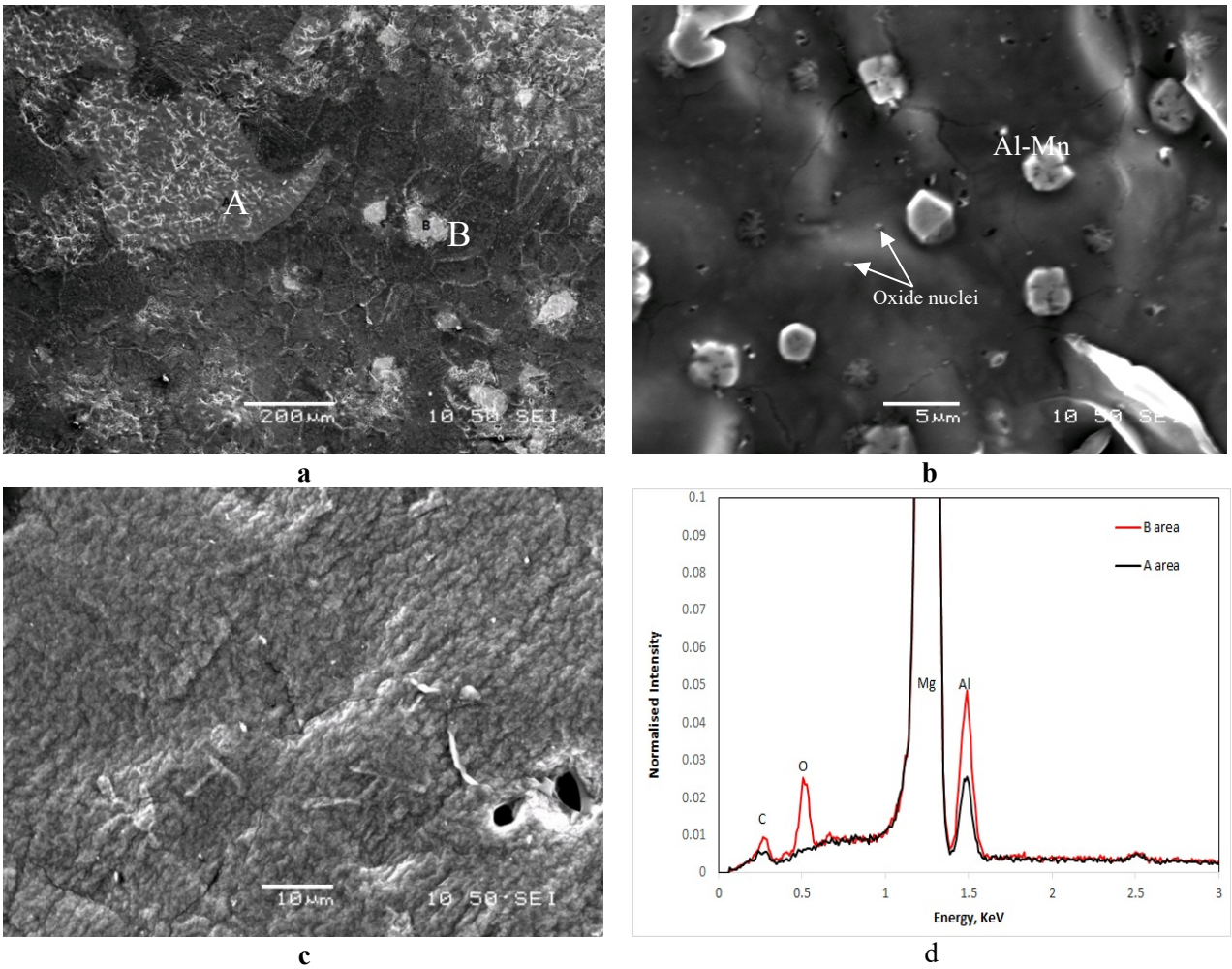

Fig. 5. SEM image from the general view of the inner surface of an entrapped UHP argon bubble in AM60B alloy: a) SE image from general view of the surface film, b) magnified view from clean part area, c) magnified view of a thick rough oxide patch area, and d) EDS spectra from clean and oxide patch areas.

[DOI: 10.22068/ijmse.1570]

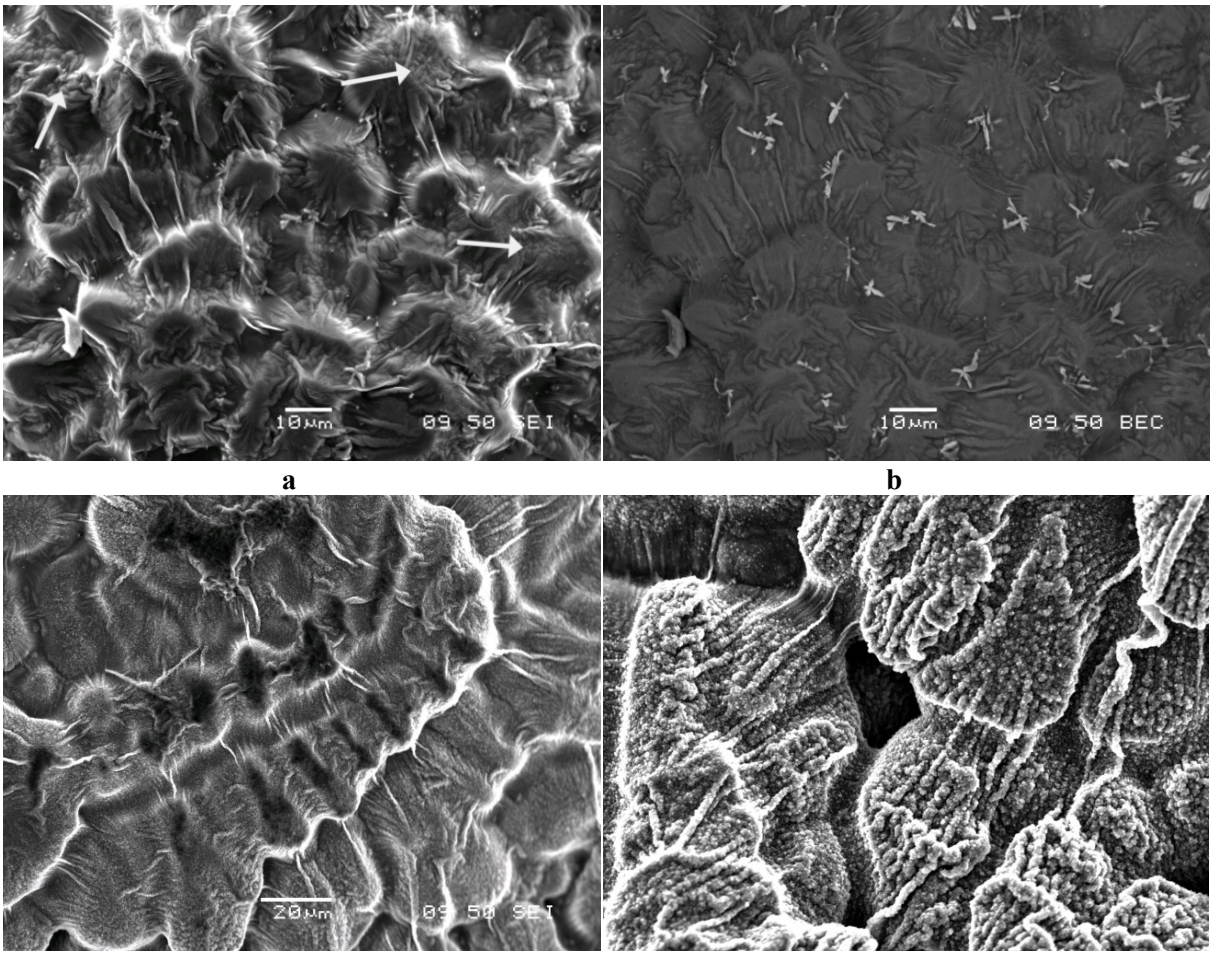

Fig. 6. Secondary electron images showing the morphology of early surface films over the solidifying structure of the molten AZ91D alloy (a,b) and AM60B alloy (c,d) formed under dry air atmosphere.

(marked by flashes in Fig. 6a) are observed due to different oxidation rate arising from inhomogeneity of chemical composition in the eutectic and solid solution areas. The script-like phases (shown in Fig. 6b) consist of Al and Mn elements according to EDS analysis. In AM60B alloy, the surface film has a rough and nodular growth morphology with some grooves and folds (as shown in Fig. 6c, d). This morphology represents a non-protective film formed due to the probable evaporation and oxidation of Mg and Al from the surface of the AM60B alloy melt.Also there is no evidence to suggest the formation of a second phase in the film. However, there are some tiny nuclei particles of MgO dispersed in the microstructure.

According to EDS analysis, the main elements attributable to the alloy and film were Mg, Al, O and a little Zn for AZ91D alloy and without Zn for AM60B alloy (e.g. Fig.2). Therefore, the oxidation product is composed of MgO and Al_2O_3 as the dominant phases. The quantitative Mg:O ratio given in AM60B alloy is less than in AZ91D alloy. Therefore, the oxide film thickness was calculated to be in the range of 15-30 nm for AZ91D alloy, and over 150 nm in AM60B alloy. As before this was determined according to calibration curves of X-ray intensity ratio against film thickness for various ratios of Mg, O and F as shown in Fig. 3 in Ref. 15.

Based on the thickness of the surface films, it can be assumed that almost all of the oxygen within the bubbles has been converted to oxide. This suggests that, there is a strong correlation between surface film thickness and its morphology. The thickness results are consistent with the formation of a relatively denser and smoother morphology film formed in AZ91D alloy compared to AM60B

[DOI: 10.22068/ijmse.1570]

alloy. As a comparison with pure magnesium alloy at the same condition, the calculated oxide film thickness was observed to cover a wide range of values, from 15 nm in thinnest film areas to 110–150 nm in top of bubble, the areas displaying a thick and folded morphology [15].

Other experimental data from the isothermal oxidation of molten AZ91D alloy at different exposure times and temperatures, showed that in the static surface film formation at 610 °C which had been exposed to air for 10 minutes, there was a predominantly elongated MgO layer with a porous sponge-like morphology, whereas after 10 seconds at 650 °C, a thin porous layer consisting of granular MgO nanoparticles was formed [12].

A plausible mechanism at the initial stage of oxidation of molten Mg-Al series alloys (AM60 and AZ91) was attributed to the high kinetic evaporation of Mg, Al and Zn. The corresponding evaporation equilibrium pressures of the elements are 6×10^{-9} mmHg for Al, 2.9 mmHg for Mg and 7.5 mmHg for Zn at 650 °C [16]. On the other hand, the ignition temperature increased with an increase in the Al concentration. It has been measured for AZ91D and AM60B alloys are 600º C and 560º C respectively [17]. Also the formation of the β-phase ($Mg_{17}Al_{12}$) in the form of a lower melting point eutectic, precipitation occurs along the grain boundaries, causes selective oxidation and accelerates the evaporation Mg. Consequently, the growth of the oxide nodules is accelerated.

It should be noted that the composition of sub-surface molten Mg alloy plays a critical role in the early oxidation resistance, so that for AM60D alloy, the concentration of Al is about 6% (mass fraction) which leads to higher oxidation rate in comparison with the AZ91D alloy (Al content of 9 wt-%).

If a single stationary bubble was to be formed instantaneously in a quiescent melt, and assuming that oxygen is the only reactive gas present, it can be concluded that at high temperatures, due to high affinity of Mg with O, oxidation products will consist of primary MgO as the dominant phase with a small amounts of Al_2O_3 and ZnO present. The remained Al could directly react with the MgO to form a spinel phase that was identified as $MgAl_2O_4$ through the below reaction (reaction 5) below. The film composition agrees with the results presented by Balart and et al. after longer times oxidation of AZ91D alloy under air atmosphere that MgO can transform into another amorphous compound $MgAl_2O_4$ [12].Shih et al. [18] showed that the $MgAl_2O_4$ spinel at the Mg-MgO interface could act as a diffusion barrier for Mg^{2+} cation:

$$Mg\ (g) + 1/2\ O_2\ (g) = MgO \quad (1)$$

$$2Al\ (l) + 3/2\ O_2\ (g) = Al_2O_3 \quad (2)$$

$$3Mg\ (l) + Al_2O_3\ (s) = 3MgO + 2Al \quad (3)$$

$$3MgO\ (s) + 2Al\ (l) = Al_2O_3 + 3Mg \quad (4)$$

$$4MgO\ (s) + 2Al\ (l) = MgAl_2O_4 + 3Mg \quad (5)$$

There are many fine and large folds observed in the early surface oxide films which have been dynamically formed over the surface of the molten Mg alloy. Some of them which appear mainly horizontal were generally associated with the growth of dendrites and have solidified relatively early and became lodged in position by adjacent solid closer to the mould wall. If the reaction rate is fast enough at the initial stage, the total gas pressure reduces during the oxidation of the inner surface of bubble and the bubble volume consequently decreases. This will also decrease the bubble surface area, causing any oxide films to buckle and fold. Consequently, as the remaining liquid solidifies and shrinks, the bubble and the surface film will expand towards the wall, allowing the oxide film to drape over the anchored solid grain. On the other hand, the solid MgO film over the molten Mg alloy has a rather different thermal expansion coefficient ($14.8\times10^{-6}\ K^{-1}$ at 725 °C for MgO and $27.2\times10^{-6}\ K^{-1}$ from 20 to 200 °C for the AZ91D alloy substrate [19]). Therefore, the expanded substrate alloy contracts more than the surface MgO layer during cooling, and this leads to folding of the surface film. Further complicating factors such as fluctuations of bubble pressure during solidification and the bubble's movement in the melt also affect the thickness, morphology and the scale of the folds in the surface film.

It has been found that the entrance of the folded oxide film as an oxide inclusion into the molten Mg alloy increases due to the volume of the entrapped air and can be considered as a criterion for assessing the seriousness of inclusion defects and their effectiveness as an initiation site for gas and shrinkage porosity in the casting. Accordingly, the detrimental effects of the folded oxide film on the mechanical properties of Mg castings have been reported before [20].

[DOI: 10.22068/ijmse.1570]

3.2.3. SF_6

Figure 7 shows the typical morphologies of the bubble surface films of AZ91D and AM60B alloys, formed under the air containing 3.5% SF_6 atmosphere. As it can be seen, a compact and uniform thickness surface film forms over dendrites, without any evidence of significant defects. The general views of SE images (Fig. 7b and 7d) clearly show that there is a wide range of grain size (ranging from 5 to 50 μm diameter).

There are also many fine granules on the surface which are precipitated within interdendritic areas (These granules were proved consist of Mg, O and F by EDS analysis).

The EDS spectra (e.g. Fig. 2) show the main elements attributed to the film and bulk alloy were Mg, Al, F, O and C elements. Also the sulphur content of the specimens exposed to SF_6 was very low compared to the oxygen and fluorine contents. The concentration of carbon in the surface film may have been resulted from the reaction between the film and ambient atmosphere, forming $MgCO_3$ as a corrosion product. Fluorine and oxygen were present in the forms of fluoride and oxide respectively. The composition of the films confirmed that MgO, MgF_2 and a little AlF_3 are the main phases present when the molten Mg-Al alloy is being protected by SF_6 mixture according to reactions 6 and 7.

$$Al_{(l)} + \frac{3}{2}F_{2_{(g)}} = AlF_3 \quad (6)$$

$$Mg_{(l)} + F_{2_{(g)}} = MgF_{2_{(s)}} \quad (7)$$

The O:F intensity ratio in the early surface films formed under SF_6 atmosphere were in the range of 0.65 in AZ91D alloy and 0.38 in AM60B alloy,

respectively. This result shows that there is a

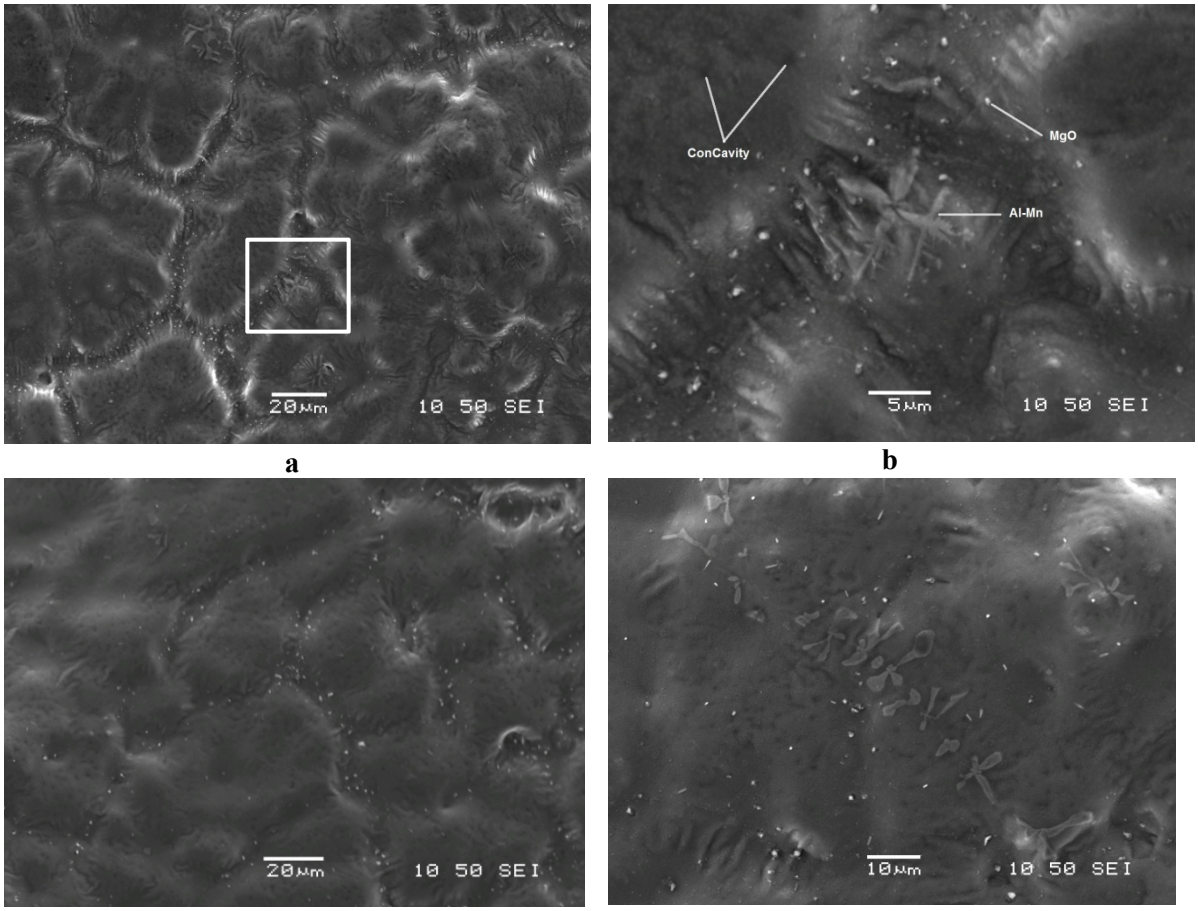

Fig. 7. SEM images of the inner surface film formed on an entrapped bubble of air/3.5%SF_6 mix in AZ91D and AM60B alloys: a,b) Secondary electron images showing typical areas in AZ91D alloy, c,d) SE images of the surface film morphology in AM60B alloy.

[DOI: 10.22068/ijmse.1570]

strong correlation between oxygen and fluorine content. Moreover, this correlation is very close to that predicted for a material with a stoichiometry of oxygen and fluorine being present in equal atomic fractions. The amount of fluoride was greater than oxide phases in the surface film for AM60B alloy.

The analysis of an isothermal experiment carried out on the molten AZ91D alloy showed that the film thickness was approximately 0.5 μm after 10 minutes exposure time under protective SF_6 atmosphere. It was also found that the O:F intensity ratio ranged from 1.62 (using 0.1%SF_6/air protective atmosphere) to 0.22 (using 1.5%SF_6/air atmosphere), suggesting the formation of a superior protective film can be achieved with higher amounts of fluoride phase in the surface film [21].

Due to the higher compactness of MgF_2 (Pilling-Bedworth or P-B ratio of 1.32) compared to MgO (P-B ratio of 0.81), a surface film with a compact morphology could be formed that provides more effective protection to the molten magnesium. The beneficial effect of MgF_2 present in MgO film probably indicates that the MgF_2 nucleation rate changes within the MgO film and/or improves wetting between the alloy and the oxide due to the presence of fluorine, as reported by Cashion [9]. It can be assumed that based on the morphology of the surface films, the oxidation rate in AZ91D and AM60B obeyed parabolic growth law under the protective SF_6 atmosphere.

3.2.4. HFC-R134a

Figure 8 shows typical SEM images of the surface films formed on the molten AZ91D and AM60B alloys under the presence of an air/3.5% HFC-R134a mixture. A compact and flat surface film is observed in the AZ91D alloy, as shown in Fig 8a and 8b. Although there are also a few thick and sponge-like patch areas identified as Mg oxides, which are probably older oxide films that were suspended in the melt and have subsequently attached themselves to the bubble (not shown in Fig. 8). The morphology of the film is similar to the very smooth and uniform surface film that was found under the same condition in the pure molten Mg alloy [15].

The early surface film of the bubble in AM60B alloy, as observed in Fig. 8c and 8d, that is not very regular. There are many irregularly distributed concavities and also small white granules on the surface (the main composition of the white granules as analyzed by EDS is Mg, O and F). The number of the white granules obviously increased (Fig. 8c), suggesting that the oxide film did not protect the AM60B melt sufficiently

The surface film is not uniform and some grooves and folds appear on its surface. These results suggest that AZ91D alloy has better oxidation resistance than AM60B alloy under an atmosphere of air containing 3.5% HFC-R134a.

The EDS spectra (e.g. Fig. 2) showed that the surface films contained Mg, Al, F, O and C. Also they indicated very similar levels of fluorine compared to the specimens prepared using air/SF_6 mixture. Oxygen levels, on the other hand are consistently lower when using HFC-R134a rather than SF_6. The film composition agrees with the results presented by Chen et al. [22] in tests using long term exposure to a similar gas composition at 760 ºC. The O:F intensity ratio was determined to be in the range of 0 - 0.2 in AZ91D alloy and 0.45-0.5 in AM60B alloy. This confirms that the film in AZ91D alloy is predominantly MgF_2, with a small amount of MgO. Furthermore, it suggests that the reaction with fluorine must be quite rapid, suppressing oxide formation at a very early stage. This indicates that an atmosphere of 3.5% HFC-R134a in dry air can provide satisfactory protection for an AZ91D alloy melt.

Chen et al. [23] reported that the oxide surface film statically formed on an AZ91D alloy under a 1%HFC-R134a/air mixture at 660 °C was a dense and compact protective layer, although it had an uneven surface with a few white MgO particles. At the higher melt temperatures, up to 800 °C, the number of white MgO particles increased and the surface film changed to a more porous and loose oxide layer. Furthermore, the average O:F intensity ratio in AZ91D at 660°C was about 0.04 and this increased to about 0.11 at 800°C which suggests that these layers are less protective at the higher temperatures.

Also it is worth mentioning that the morphology of the secondary intermetallic phase, containing Al-Mn, formed under HFC-R134a atmosphere is a script-like shape as shown in Fig. 8b and 8d. This could be due to the fact that the surface film formation was very quick and there was no sufficient time for the formation of with the usual shape.

[DOI: 10.22068/ijmse.1570]

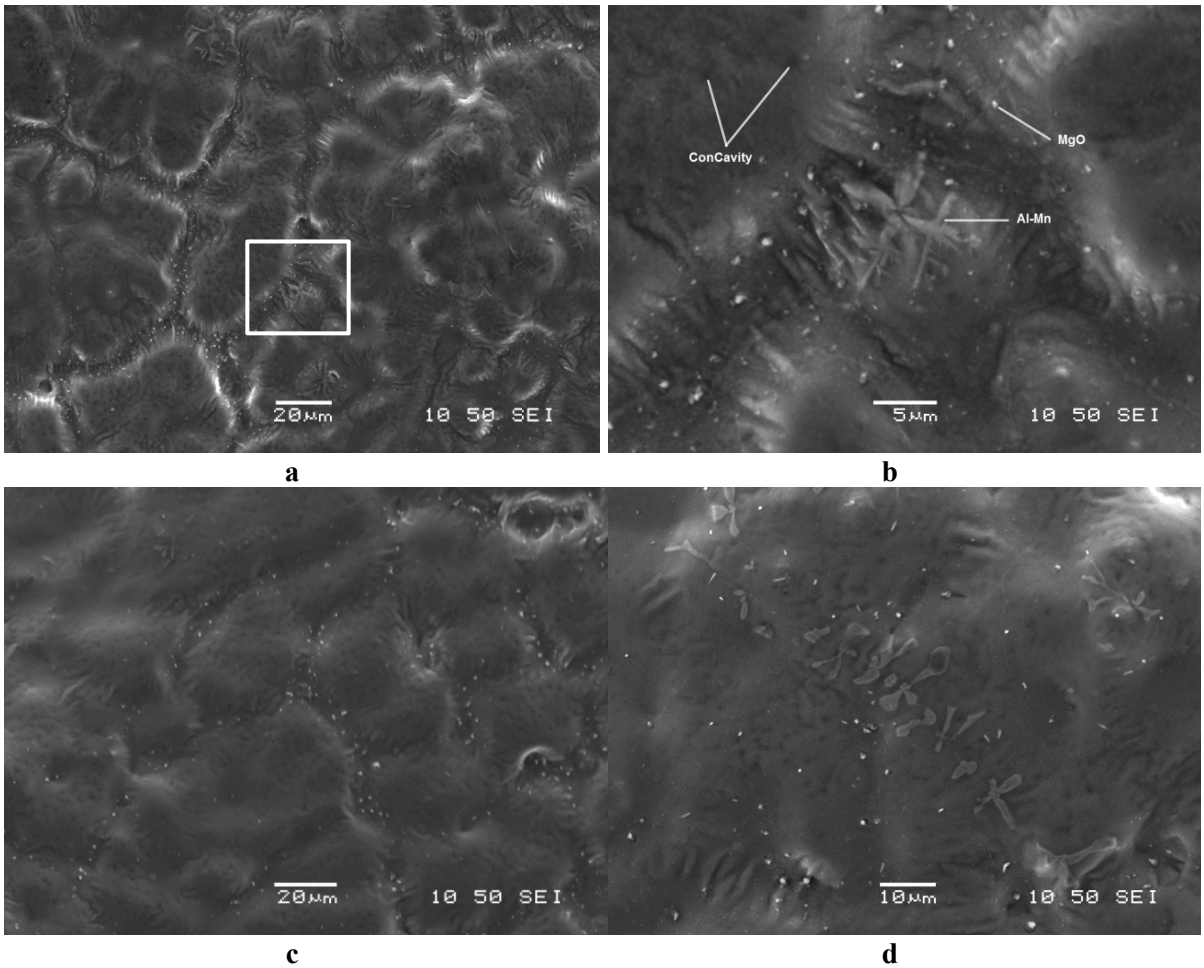

a b c d

Fig. 8. SEM image from the general view of the inner surface of an entrapped UHP argon bubble in AM60B alloy: a) SE image from general view of the surface film, b) magnified view from clean part area, c) magnified view of a thick rough oxide patch area, and d) EDS spectra from clean and oxide patch areas..

4. CONCLUSIONS

1- The early surface film formed on the molten Mg alloy (in terms of thickness, morphology and composition) is strongly affected by the gas composition and the vapor pressure of alloy. A strong link was found between the oxidation kinetics and the film morphology.

2- Due to a very low reactivity of UHP-argon with the melt, the majority of the surface is very clean which suggests that the observed oxide growth is subsequent and occurs in the solid state after solidification in AZ91D alloy. The surface film in AM60B alloy consists of rough and folded oxide patches. It seems that the molten AM60B alloy is therefore more sensitive to the effects of impurities under UHP-argon than the AZ91D alloy.

3- A uniform surface oxide layer covers the melt surface structure of the AZ91D alloy under dry air atmosphere in early stages of oxidation. For AM60B alloy, the surface film has nodular growth morphology. According to EDS analysis, the main elements in the surface films of both alloys are identified as Mg, Al and O. Also in the surface film formed in AM60B alloy, the oxygen content increased. it is concluded that the composition of the sub-surface molten Mg alloy plays a critical role in the early oxidation resistance, so that for AM60D alloy, due to less concentration of Al which leads to a higher oxidation rate in comparison with the AZ91D alloy.

4- The Mg:O ratio from the EDS spectra of the early surface film formed under dry air atmosphere indicates that the thickness of MgO

[DOI: 10.22068/ijmse.1570]

films varies uniformly in range 15 - 30 nm in AZ91D and up to 150 nm in AM60B alloy. This confirms that, there is a strong correlation between film morphology and its thickness. The small numbers of discrete oxide particles are assumed to have created laterally over the melt surface.

5- A thin, continuous and dense surface film was formed under an SF_6 /dry air mixture atmosphere (at the concentrations used in this work, i.e. 3.5 vol.%) in both AZ91D and AM60B alloys. The main elements attributed to the film and bulk alloy were Mg, Al, F, O and C elements. The O:F intensity ratios observed in the early surface films were in the range 0.65 in AZ91D alloy and 0.38 in AM60B alloy respectively. This result shows that there is a strong correlation between oxygen and fluorine content under SF_6 /dry air atmosphere.

6- A compact and uniformly flat surface film of predominantly MgF_2 is formed in the AZ91D alloy in the presence of an air/3.5% HFC-R134a mixture. This result is supported with the O:F ratio that was in range of 0-0.2. In addition to the MgF_2, there are small amounts of MgO and AlF_3. While, in the AM60D alloy, the surface film was non-uniform with some grooves and folds on its surface. The results show that AZ91D alloy has better oxidation resistance than AM60B alloy under the atmosphere of air containing HFC-R134a at 3.5 vol% concentration.

5. ACKNOWLEDGEMENTS

The author wish to thank to John Taylor at the CAST Cooperative Research Centre and CSIRO Materials Science and Engineering in Brisbane, Australia, for helping to carry out the research program and revising in grammatically corrections.

6. REFERENCES

[1] Avedesian, M. and Baker, H., ASM Specialty Handbook: Magnesium and Magnesium Alloys, ASM International, 1999, 250-300.

[2] Pettersen, G., Vrelid, E., Tranell, G., Fenstad, J., Gjestland, H., Characterization of the surface films formed on molten magnesium in different protective atmospheres, Materials Science and Engineering, 2002, A332 , 285–294

[3] Cashion, S.P., Ricketts, N.J., Hayes, P.C., The mechanism of protection of molten magnesium by cover gas mixtures containing sulphur hexafluoride, Light Metals, 2002, 2, 43–47.

[4] Mirak, A.R., Divandari, M., Boutorabi, S.M.A. and Taylor, J.: Effect of oxide film defects generated during mould filling on mechanical strength and reliability of magnesium alloy castings (AZ91), Cast Metals Res., 2012, 20, 215–220.

[5] Couling, S.L., Bennett, F.C., Leontis, T.E., Melting magnesium under air/SF6 protective atmospheres, Light Metal Age, 1977, 35, 12–21.

[6] Arestad, K., Tranell, G., Petterson, G. and Abel Engh, T., Various techniques to study the surface of magnesium protected by SF6, Magnesium Technology , 2003 , TMS, 2003.

[7] Chen, H.K., Liu, J. R.and Huang, W.D., Characterization of the protective surface films formed on molten magnesium in air/R134a atmospheres, Materials Characterization, 2007, 58, 51–58.

[8] Zhao, L., Liu, J. R, Chen, H. K. and Huang, W.D. The characterization of surface films formed on molten magnesium and AZ91D alloy in air/1,1,1,2-tetrafluoroethane atmosphere, Alloys and Compound, 2009, 480, 711–716.

[9] Ricketts, N. J., Cashion, S.P., Bailey, R., Industrial trials with the AM Cover gas system for magnesium melt protection, in: Proceedings of the Light Metals Technology Conference, 2003. 286-295.

[10] Cheng, C., Lan, Q., Wang, A., Le, Q., Yang, F. and Li, X., Effect of Ca Additions on Ignition Temperature and Multi-Stage Oxidation Behavior of AZ80, Metals 2018, 8, 766-775.

[11] Czerwinski, F., The early stage oxidation and evaporation of Mg–9%Al–1%Zn alloy Corrosion Science, 2004, 46, 377–386.

[12] Balart M. J. and Fan Z., Surface oxidation of molten AZ91D magnesium alloy in air, Cast Metal Research, 2014, 27, No. 3, 167-176.

[13] Czerwinski, F., 'The oxidation behaviour of an AZ91D magnesium alloy at high temperatures, Acta Materialia, 2002, 50, 2639–2654.

[14] Liu, J.R., Chen, H.K., Zhao, L., Huang, W.D., Oxidation behaviour of molten magnesium and AZ91 alloy in 1,1,1,2-tetrafluoroethane/air atmospheres, Corrosion Science 2009, 51,

[DOI: 10.22068/ijmse.1570]

129–134.
[15] Mirak, A.R., Davidson, C.J., Taylor, J.A., Characterization of fresh surface oxidation films formed on pure molten magnesium in different atmospheres, Corrosion Science 2010, 52, 1992–2000.
[16] Ha W. and Kim Y.J., 'Effects of cover gases on melt protection of Mg alloys' Alloys Compd, 2006, 422, 208–213.
[17] Ming, L., Donald, S. Shih, b, Catherine, P. c, Andrej, A., The ignition temperature of Mg alloys WE43, AZ31 and AZ91, Corrosion Science, 2012, 54, 139–142.
[18] Shih T. S., Liu J. B., and Wei P. S., Oxide films on magnesium and magnesium alloys, Mater. Chem. Phys. 2007, 104, 497–504.
[19] Balart, M. J., Patel J. B. and Fan Z., Melt Protection of Mg-Al Based Alloys, Metals, 2016, 6, 131-139.
[20] Mirak, A.R., Divandari, M., Boutorabi, S.M.A. and Campbell, J.: Oxide film characteristics of AZ91 magnesium alloy in casting conditions, Int. J. Cast Metals Res., 2007, 20, 215–220.
[21] Xiong, S.M. and Liu, X.L., Microstructure, composition and depth analysis of surface films formed on molten AZ91D alloy under protection of SF6 mixtures, Met. Mat. Trans. A, 2007, 428-434.
[22] Chen, H., Effect of melt temperature on the oxidation behavior of AZ91 magnesium alloy in air/HFC-R134a atmospheres, Material Characterization, 2010, 61, 894 – 898.
[23] Chen, H., Jianrui. L., Huang, W., Oxidation behavior of molten magnesium in air/HFC-R134a atmospheres, J Mater Sci, 2006, 41, 8017–8024.

[DOI: 10.22068/ijmse.1570]